Journal of Thermal Analysis and Calorimetry, Vol. 76 (2004) 217–225

THERMAL DECOMPOSITION OF SYNTHETIC HYDROTALCITES REEVESITE AND PYROAURITE

R. L. Frost and K. L. Erickson*

Inorganic Materials Research Program, School of Physical and Chemical Sciences, Queensland University of Technology, GPO Box 2434, Brisbane Queensland 4001, Australia

(Received October 16, 2003; in revised form December 10, 2003)

Abstract

A combination of high resolution thermogravimetric analysis coupled to a gas evolution mass spectrometer has been used to study the thermal decomposition of synthetic hydrotalcites reevesite ($Ni_6Fe_2(CO_3)(OH)_{16}\,4H_2O$) and pyroaurite ($Mg_6Fe_2(SO_4,CO_3)(OH)_{16}\,4H_2O$) and the cationic mixtures of the two minerals. XRD patterns show the hydrotalcites are layered structures with interspacing distances of around 8.0 Å. A linear relationship is observed for the *d*(001) spacing as Ni is replaced by Mg in the progression from reevesite to pyroaurite. The significance of this result means the interlayer spacing in these hydrotalcites is cation dependent. High resolution thermal analysis shows the decomposition takes place in 3 steps. A mechanism for the thermal decomposition is proposed based upon the loss of water, hydroxyl units, oxygen and carbon dioxide.

Keywords: dehydration, dehydroxylation, high-resolution thermogravimetric analysis, hydrotalcite, pyroaurite, reevesite

Introduction

The discovery of large amounts of natural hydrotalcites at Mount Keith in Western Australia means that these minerals could be mined for specific applications. Further a wide range of hydrotalcites based on sulphate, chloride and carbonate have been found in the MKD5 Nickel deposit, Mount Keith, Western Australia (Details from Dr Ben A. Grguric, Senior Project Mineralogist, Western Mining Corporation). In order to understand the complex relationships between iowaite/pyroaurite, stichite/woodallite and hydrotalcite/mountkeithite series, it is necessary to study the synthetic minerals. Interest in the study of these hydrotalcites results from their potential use as catalysts, adsorbents and anion exchangers [1–5]. The reason for the potential application of hydrotalcites as catalysts rests with the ability to make mixed metal oxides at the atomic level, rather than at a particle level. Such mixed metal oxides are formed through the thermal decomposition of the hydrotalcite [6, 7]. The minerals at Mount

* Author for correspondence: E-mail: r.frost@qut.edu.au

1388–6150/2004/ $ 20.00

Akadémiai Kiadó, Budapest
Kluwer Academic Publishers, Dordrecht

Keith may have economic value for these purposes. Hydrotalcites may also be used as components in new nano-materials such as nano-composites [8]. Incorporation of low levels of hydrotalcite into polymers enables polymeric materials with new and novel properties to be manufactured. There are many other uses of hydrotalcites. Hydrotalcites are important in the removal of environmental hazards in acid mine drainage [9, 10]. Hydrotalcite formation also offer a mechanism for the disposal of radioactive wastes [11]. Hydrotalcite formation may also serve as a mean of heavy metal removal from contaminated waters [12]. Recently Frost *et al*. showed the thermal analysis patterns of several natural hydrotalcites namely carrboydite and hydrohonessite obtained from mineral deposits in Western Australia. These hydrotalcites are readily synthesised by a co-precipitation method [13–15].

Hydrotalcites, or layered double hydroxides (LDH's) are fundamentally anionic clays, and are less well-known than cationic clays like smectites [16, 17]. The structure of hydrotalcite can be derived from a brucite structure ($Mg(OH)_2$) in which e.g. Al^{3+} or Fe^{3+} (pyroaurite-sjögrenite) substitutes a part of the Mg^{2+}. In the case of the Mount Keith deposits, reevesite, hydrotalcite, mountkeithite and pyroaurite predominate. Further mixtures of these mineral phases with multiple anions in the interlayer are observed. This substitution creates a positive layer charge on the hydroxide layers, which is compensated by interlayer anions or anionic complexes [18, 19]. In hydrotalcites a broad range of compositions are possible of the type $[M^{2+}_{1-x}M^{3+}_{x}(OH)_2][A^{n-}]_{x/n}\,yH_2O$, where M^{2+} and M^{3+} are the di- and trivalent cations in the octahedral positions within the hydroxide layers with x normally between 0.17 and 0.33. A^{n-} is an exchangeable interlayer anion [20]. In the hydrotalcites reevesite and pyroaurite, the divalent cations are Ni^{2+} and Mg^{2+} respectively with the trivalent cation being Fe^{3+}. In these cases the carbonate anion is the major interlayer counter anion. There exists in nature a significant number of hydrotalcites which are formed as deposits from ground water containing Ni^{2+} and Fe^{3+} [21]. These are based upon the dissolution of Ni–Fe sulphides during weathering. Among these naturally occurring hydrotalcites are reevesite and pyroaurite [22, 23]. Related to hydrohonessite is the mineral mountkeithite in which all or part there of, the Ni^{2+} is replaced by Mg^{2+}. These hydrotalcites are based upon the incorporation of carbonate into the interlayer with expansions of around 8 Å. Normally the hydrotalcite structure based upon takovite (Ni,Al) and hydrotalcite (Mg,Al) has basal spacings of ~8.0 Å where the interlayer anion is carbonate. If the carbonate is replaced by sulphate then the mineral carboydite is obtained. Similarly reevesite is the Ni,Fe hydrotalcite with carbonate as the interlayer anion, which when replaced by sulphate the minerals honessite and hydrohonessite are obtained.

The use of thermal analysis techniques for the study of the thermal decomposition of hydrotalcites is not common [24]. Heating sjögrenite or pyroaurite at <200°C caused the reversible loss of H_2O. At 200–250°C on static heating, or 200–350°C on dynamic heating, very little H_2O or CO_2 were lost, but changes in the infrared spectrum and DTA effects were observed [24]. Recently thermal analysis techniques have been applied to some complex mineral systems [25–27]. To date the number of thermal analysis studies of these minerals is very limited. Recent thermal analysis studies of the natural minerals were complicated by the formation of mixed anionic species; i.e. a mixture

of reevesite and pyroaurite was formed. In this work we have synthesised these minerals and now report the thermal analysis of synthetic reevesite and pyroaurite.

Experimental

Synthetic minerals

Minerals were synthesised by the co-precipitation method. Hydrotalcites with a composition of $(Ni,Mg)_6Fe_2(OH)_{16}(CO_3)\ 4H_2O$ were synthesised. Three solutions were prepared. Solution 1 contained 2 M NaOH and 0.125 M Na_2CO_3, solution 2 contained 0.75 M Ni^{2+} ($Ni(NO_3)_2\ 6H_2O$) and solution 3 contained 0.75 M Mg^{2+} ($Mg(NO_3)_2\ 6H_2O$) in the appropriate ratio, together with 0.25 M Fe^{3+} (as $(Fe(NO_3)_3\ 9H_2O)$) . Solution 2 in the appropriate ratio was added to solution 1 using a peristaltic pump at a rate of 40 $cm^3\ min^{-1}$, under vigorous stirring, maintaining pH 10. The precipitated minerals were washed at ambient temperatures thoroughly with water to remove any residual nitrate. This step is important as the slightest trace of nitrate as sodium nitrate is readily evident in the synthesised hydrotalcite. If the solution 2 contains Ni^{2+} and combined with solution 1, then the mineral reevesite is formed; if the solution 3 containing Mg^{2+} is added to solution 1, then pyroaurite is formed. The composition of the hydrotalcites was determined by electron probe analyses. The phase composition was checked by X-ray diffraction.

Thermal analysis

Thermal decomposition of the hydrotalcite was carried out in a TA® Instruments incorporated high-resolution thermogravimetric analyzer (series Q500) in a flowing nitrogen atmosphere (80 $cm^3\ min^{-1}$). Approximately 50 mg of sample was heated in an open platinum crucible at a rate of 2.0°C min^{-1} up to 500°C. The heating program of the instrument was regulated precisely to provide a uniform rate of decomposition in the main decomposition stage. The TGA instrument was coupled to a Balzers (Pfeiffer) mass spectrometer for gas analysis. Only selected gases were analyzed.

Results and discussion

X-ray diffraction

The X-ray diffraction patterns of the synthesised reevesite and mixed cationic reevesite are shown in Fig. 1. The XRD patterns clearly show the hydrotalcites are layered structures with interspacing distances of around 8.0 Å. The XRD patterns for the reevesite patterns are less noisy; this is attributed to the crystallinity of the reevesite phase. The reevesite crystallises more rapidly than pyroaurite. Such a phenomena can be observed in the width of the XRD peaks. The *d*(001) peak for reevesite is sharp, whereas the peaks for the pyroaurites are broad.

Variations in the *d*(001) spacing are observed (Fig. 2). An almost linear variation is observed as Ni is replaced by Mg in the progression from reevesite to pyroaurite. The

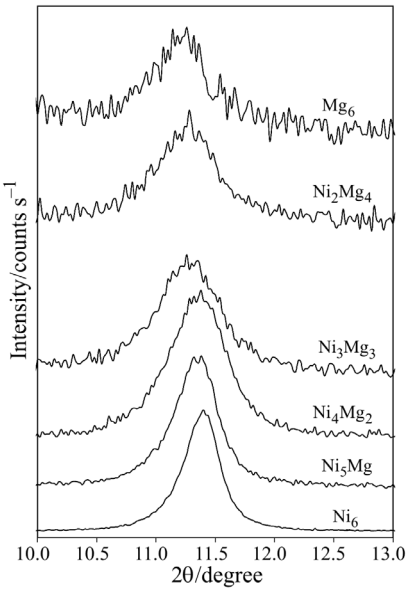

Fig. 1 X-ray diffraction patterns of the d(001) spacing of reevesite-pyroaurite

equation is y=0.0202x+7.7845 with R^2=0.9914. The significance of this result is that not only are the interlayer spacing of hydrotalcites anion dependent [28] but are also cation dependent. Synthetic reevesite ($Ni_6Fe_2(SO_4)(OH)_{16}\,4H_2O$) has a d spacing of 7.78 Å; when one mole of Ni is replaced with Mg, the synthetic reevesite of formula ($(Mg,Ni_5)Fe_2(SO_4)(OH)_{16}\,4H_2O$) has a d spacing of 7.81 Å. The Mg end member

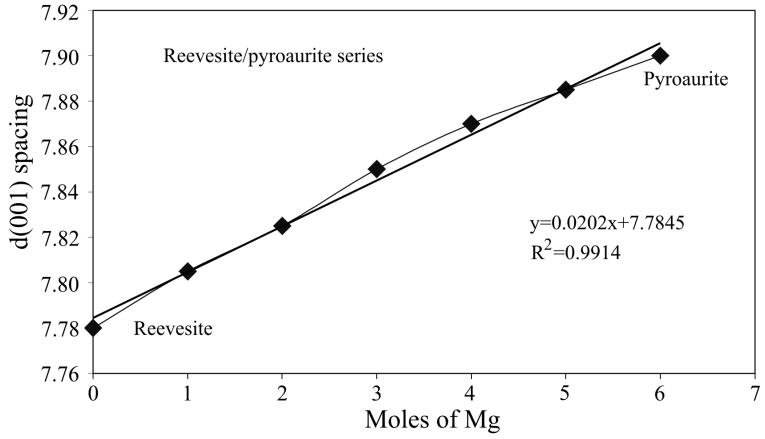

Fig. 2 Variation of the d(001) spacing with magnesium content (reevesite to pyroaurite)

(pyroaurite) has a *d*(001) spacing of 7.91 Å. Figure 2 also reflects the strength of the bonds formed between the NiOH units and the carbonate. The bond strength is much stronger for the reevesite compared with pyroaurite.

Thermogravimetric analysis and mass spectrometric analysis

The high resolution thermogravimetric analysis (HRTG) for the synthetic reevesite-pyroaurite series are shown in Fig. 3. The evolved gas mass spectrometric curves are shown in Fig. 4. These plots are representative ones and typify the MS curves

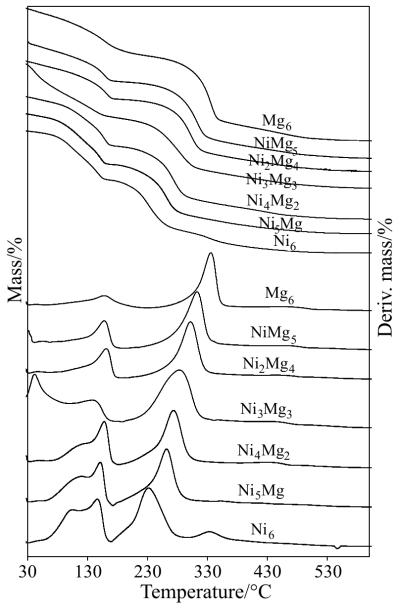

Fig. 3 TG and DTG curves for reevesite-pyroaurite

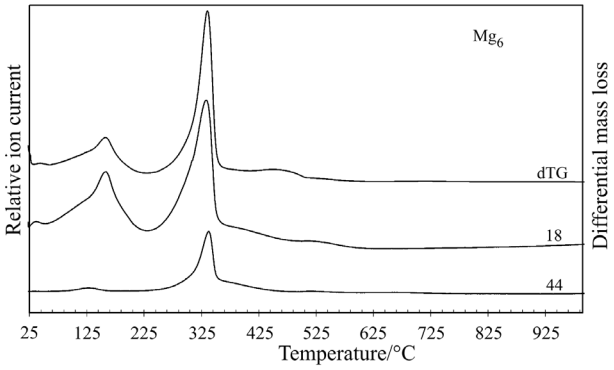

Fig. 4 DTG and MS curves for pyroaurite (as an example)

Table 1 Results of the HRTG of synthetic reevesite-pyroaurite

Reevesite/ Pyroaurite	Step 1: dehydration			Step 2: dehydroxylation, de-carbonation			Step 3: de-oxygenation		
	Mass loss/%		Temp./°C	Mass loss/%		Temp./°C	Mass loss/%		Temp./°C
	found	theor.		found	theor.		found	theor.	
Ni_6	14.15	8.30	150	15.30	13.37	248	5.58	3.47	341
Ni_5Mg	14.04	8.64	154	15.57	13.92	266	4.93	3.61	353
Ni_4Mg_2	12.81	9.01	163	17.62	14.52	279	4.96	3.75	377
Ni_3Mg_3	13.76	9.42	146	17.34	15.17	290	5.56	3.91	390
Ni_2Mg_4	11.33	9.86	165	17.59	15.88	307	3.15	4.08	404
$NiMg_5$	11.28	10.35	161	17.15	16.67	320	4.95	4.27	438
Mg_6	13.94	10.88	158	19.58	17.53	336	4.92	4.47	455

Table 2 Results of the evolved gas mass spectrometry of synthetic reevesite-pyroaurite

Reevesite/Pyroaurite	Temperature/°C		
	Dehydration	Dehydroxylation De-carbonation	De-oxygenation
Ni_6	148	234	342
Ni_5Mg	152	264	363
Ni_4Mg_2	159	278	438
Ni_3Mg_3	140	283	421
Ni_2Mg_4	167	307	458
$NiMg_5$	161	314	465
Mg_6	162	338	459

obtained in this work. The results of the analyses of the mass loss and temperature of the mass loss are reported in Table 1. The temperatures of the evolved gas MS mass gain are reported in Table 2. Several mass loss steps are observed. A mass loss step is observed over the 158 to 168°C temperature range and is attributed to the mass loss due to dehydration. A second mass loss step is observed over the 230 to 340°C temperature range and is attributed to dehydroxylation. The third mass loss occurs from 340 to 460°C, and is attributed to a loss of oxygen. The mass loss for dehydration takes place in two steps for the reevesite with two dehydration steps at temperatures of 103 and 150°C, for the one mole of Mg substituted reevesite the dehydration mass loss steps occur at 110 and 154°C and for the two moles of Mg substituted reevesite dehydration mass loss steps occur at 121 and 163°C. For the equimolar Mg–Ni reevesite/pyroaurite dehydration extends over a wide temperature range; no two distinct DTG maxima are observed and the maximum is observed at 146°C. This particular hydrotalcite appears to be different from the remainder of the series. One possibility is that there is not a regular cation

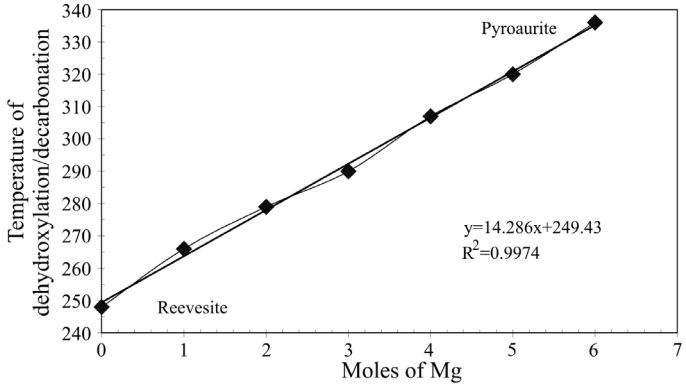

Fig. 5 Variation of the temperature of dehydroxylation with magnesium content (reevesite to pyroaurite)

distribution of Mg and Ni but cationic groups may be formed. The temperature of dehydration for the pyroaurite end members the temperature changes from 165°C for Ni_2Mg_4 to 161°C for $NiMg_5$ and 158°C for pyroaurite. The temperature of dehydration appears to increase then decrease in the series form reevesite to pyroaurite. The same trend is observed in the temperatures for mass gain due to evolved water vapour (Table 2). Table 1 shows the experimental mass losses due to dehydration and a comparison is made with the theoretical mass losses based upon a formula for the reevesite/pyroaurite based upon 16 mol of water. Such a result is not unexpected as hydrotalcites can adsorb water.

Table 1 shows the temperature for the dehydroxylation and decarbonation. Figure 4 shows that the water and carbon dioxide are evolved simultaneously. The temperatures of dehydroxylation as determined by the evolved water vapour are in excellent agreement with the HRTG results. The temperature of dehydroxylation increases linearly in the reevesite-pyroaurite series (Fig. 5). The temperature of dehydroxylation reflects the strength of the bond between the cation and the hydroxyl groups. The experimental mass loss steps for dehydroxylation/decarbonation are in reasonable agreement with theoretical mass loss calculations. The temperatures as determined by MS are higher than those from HRTG.

Mechanism for the thermal decomposition of reevesite-pyroaurite series

The following set of steps show the mass loss steps, the temperature of the mass loss and the chemical reaction associated with the mass loss:

Step 1 Temperature range 150 to 165°C

$$(Ni_{(6-x)}Mg_x)Fe_2(CO_3)(OH)_{16}\ 4H_2O \quad (Ni_{(6-x)}Mg_x)Fe_2(CO_3)(OH)_{16}+4H_2O$$

Step 2 Temperature range 245 to 340°C

$$(Ni_{(6-x)}Mg_x)\ Fe_2(CO_3)(OH)_{16} \quad (Ni_{(6-x)}Mg_x)O_5Fe_2O_3+CO_2+8H_2O$$

Step 3 Temperature range 341–455°C

$$(Ni_{(6-x)}Mg_x)O_5Fe_2O_3 \quad (Ni_{(6-x)}Mg_x)Fe_2O_3+O_2$$

The first step represents the dehydration step with the consequent loss of water. This step occurs in general over the 150 to 165°C temperature range. The second step involves the simultaneous loss of carbon dioxide and water. It is assumed that the metal oxides are formed. The third mass loss step involves oxygen loss and the reduction in the moles of oxygen in the mixed metal oxide.

Conclusions

The HRTGA of the two related minerals reevesite and pyroaurite have been studied. These hydrotalcite minerals show at least five mass loss steps ascribed to
(a) water-desorption; (b) dehydration; (c) dehydroxylation; (d) loss of oxygen; (e) de-carbonating.

HRTG shows that (a) the temperature of dehydration increases with increased substitution. The temperature increases for Mg_3Ni_3 and then decreases. (b) The temperature of dehydroxylation increases as the Mg content is increased. (c) The temperature for the loss of hydroxyl/carbonate increases with Mg content. Mechanisms for the thermal decomposition of the reevesite-pyroaurite series are proposed. The effect of cation substitution increases the interlayer distance.

References

1 J. T. Kloprogge and R. L. Frost, Applied Catalysis, A: General, 184 (1999) 61.
2 A. Alejandre, F. Medina, X. Rodriguez, P. Salagre, Y. Cesteros and J. E. Sueiras, Appl. Catal., B, 30 (2001) 195.
3 J. Das and K. Parida, React. Kinet. Catal. Lett., 69 (2000) 223.
4 S. H. Patel, M. Xanthos, J. Grenci and P. B. Klepak, J. Vinyl Addit. Technol., 1 (1995) 201.
5 V. Rives, F. M. Labajos, R. Trujillano, E. Romeo, C. Royo and A. Monzon, Appl. Clay Sci., 13 (1998) 363.
6 F. Rey, V. Fornes and J. M. Rojo, J. Chem. Soc., Faraday Trans., 88 (1992) 2233.
7 M. Valcheva-Traykova, N. Davidova and A. Weiss, J. Mater. Sci., 28 (1993) 2157.
8 C. O. Oriakhi, I. V. Farr and M. M. Lerner, Clays and Clay Minerals, 45 (1997) 194.
9 G. Lichti and J. Mulcahy, Chemistry in Australia, 65 (1998) 10.
10 Y. Seida and Y. Nakano, J. Chem. Eng. Japan, 34 (2001) 906.
11 Y. Roh, S. Y. Lee, M. P. Elless and J. E. Foss, Clays and Clay Minerals, 48 (2000) 266.
12 Y. Seida, Y. Nakano and Y. Nakamura, Water Research, 35 (2001) 2341.
13 M. A. Aramendia, V. Borau, C. Jimenez, J. M. Marinas, J. M. Luque, J. R. Ruiz and F. J. Urbano, Mater. Lett., 43 (2000) 118.
14 V. R. L. Constantino and T. J. Pinnavaia, Inorg. Chem., 34 (1995) 883.
15 M. Del Arco, P. Malet, R. Trujillano and V. Rives, Chem. Mater., 11 (1999) 624.
16 K. Hashi, S. Kikkawa and M. Koizumi, Clays and Clay Minerals, 31 (1983) 152.
17 L. Ingram and H. F. W. Taylor, Mineralogical Magazine and Journal of the Mineralogical Society, (1876–1968) 36 (1967) 465.
18 R. M. Taylor, Clay Minerals, 17 (1982) 369.
19 H. F. W. Taylor, Mineralogical Magazine and Journal of the Mineralogical Society, (1876–1968) 37 (1969) 338.
20 H. C. B. Hansen and C. B. Koch, Applied Clay Science, 10 (1995) 5.
21 E. H. Nickel and J. E. Wildman, Mineralogical Magazine, 44 (1981) 333.
22 D. L. Bish and A. Livingstone, Mineralogical Magazine, 44 (1981) 339.
23 E. H. Nickel and R. M. Clarke, American Mineralogist, 61 (1976) 366.
24 P. G. Rouxhet and H. F. W. Taylor, Chimia, 23 (1969) 480.
25 R. L. Frost, Z. Ding and H. D. Ruan, J. Therm. Anal. Cal., 71 (2003) 783.
26 R. L. Frost, W. Martens, Z. Ding and J. T. Kloprogge, J. Therm. Anal. Cal., 71 (2003) 429.
27 E. Horvath, R. L. Frost, E. Mako, J. Kristof and T. Cseh, Thermochim. Acta, 404 (2003) 227.
28 W. N. Martens, Z. Ding, R. L. Frost, J. Kristof and J. T. Kloprogge, J. Raman Spectroscopy, 33 (2002) 31.